International Journal of Control, Automation and Systems 16(X) (2018) 1-11
http://dx.doi.org/10.1007/s12555-016-0741-z
ISSN:1598-6446 eISSN:2005-4092
http://www.springer.com/12555

Formation Control of Swarm Robots with Multiple Proximity Distance Sensors

Kazunori Sakurama*, Yusuke Kosaka, and Shin-ichiro Nishida

Abstract: This study deals with the formation control problem of swarm robots using position sensitive detector (PSD) proximity distance sensors based on light-emitting diodes (LEDs). These proximity distance sensors are lightweight and quickly responsive, and are expected to enhance the mobility and flexibility of swarm robots. However, as each sensor has a narrow detection angle, the formation control problem becomes more difficult than when wide-directional distance sensors (such as cameras and laser rangefinders) are used. To overcome this difficulty, we design a two-part motion controller that controls both position and attitude. The attitude controller is necessary for continuous detection of other robots through the narrow detection angles. The designed controller is distributed in the sense that it requires only information on measured values of each robot's own sensors. Next, we derive an appropriate sensor arrangement (positions and detection angles) that achieves the desired formation pattern. Finally, the effectiveness of the proposed method is demonstrated in an experiment performed by six omni-wheeled robots equipped with LED-based PSD proximity distance sensors.

Keywords: Distributed control, formation control, proximity distance sensors, swarm robotics.

1. INTRODUCTION

Autonomous robots are being increasingly deployed in hazardous environments such as sea floats, seafloors, and fire sites [1–4]. The deployment of multiple robots at these sites would improve the efficiency of the operation. Multiple robots are applicable to a wide range of engineering problems; the monitoring and surveillance of forest fires, search and rescue of disaster victims by multiple unmanned aerial vehicles (UAVs) [5, 6], ocean sampling, mapping, and communication by multiple autonomous underwater vehicles (AUVs) [7, 8], observations of the geomagnetic field and plasmas by cluster satellites [9, 10], and many more.

For accurate detection and observation, multiple robots must maintain a rigid formation. Formation control, which control engineers have vigorously studied for decades [11–16], ensures that multiple robots keep their relative positions (distances and directions) from neighboring robots, and thus maintain the desired formation shape. Existing studies assume that to measure the relative positions each robot is equipped with wide-directional (or omni-directional) sensors such as cameras and laser rangefinders [17–21]. However, these sensors increase the weight and cost, and slow the response of the system, either by their physical limitations or through the data processing. To enhance the mobility, flexibility, and ease of introduction of swarm robots, we should attempt formation control by lighter, cheaper, and faster sensor systems.

For this purpose, we employ position sensitive detector (PSD) proximity distance sensors based on light-emitting diodes (LEDs) [22, 23]. Besides being cheap and lightweight, these proximity distance sensors detect nearby objects only in certain directions, enabling fast and simple information processing. However, due to this property, these sensors have a narrow detection angle, which can be a drawback. The detection angles of LED-based PSD proximity distance sensors and conventional wide-angle sensors are compared in Fig. 1, where Robot A is equipped with proximity distance sensors with narrow detection angles in (a) and (a'), while it is equipped with wide-directional distance sensors in (b) and (b'). In cases (a) and (b), Robot A can detect Robots B and C. However, in case (a'), where Robot A slightly rotates from (a), Robot A cannot detect the other robots because of the narrow detection angles while it can in (b') due to the wide detection angles. In this way, by using proximity distance sensors, the information on the other robots is possibly lost dependently on the robot attitude. This makes the formation control more difficult than wide-directional distance sensors, which provides information independently of the attitude. See Appendix A for more comparison.

Manuscript received November 29, 2016; revised February 1, 2017 and April 4, 2017; accepted May 28, 2017. Recommended by Associate Editor Hyo-Sung Ahn under the direction of Editor Yoshito Ohta. This work was partly supported by JSPS KAKENHI Grant Number 15K06143.

Kazunori Sakurama, Yusuke Kosaka, and Shin-ichiro Nishida are with Graduate School of Engineering, Tottori University, 4-101 Koyama-Minami, Tottori-shi, Tottori 680-8552, Japan (e-mails: {sakurama@mech, M14T1008U@edu, nishida@mech}.tottori-u.ac.jp).
* Corresponding author.

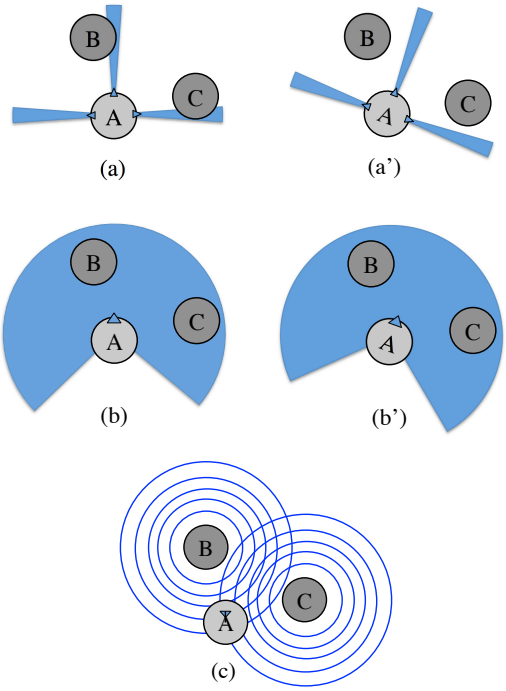

Fig. 1. Detection angles of distance sensors: (a), (a') proximity distance sensors; (b), (b') wide-angle distance sensors; (c) range-only distance sensors.

To overcome this difficulty, we propose a two-part motion controller that controls both position and attitude. The problem of the narrow detection angle is solved by the attitude controller, which enables each robot to continuously detect other robots by proximity distance sensors. The designed controller is distributed in the sense that it requires only the information from each robot's own sensors, which is naturally derived by the gradient-flow approach [24–26]. Next, an appropriate sensor arrangement (positions and detection angles) that achieves the desired formation is given. Finally, the effectiveness of the proposed method is demonstrated through an experiment performed by six omni-wheeled robots equipped with LED-based PSD proximity distance sensors.

Formation control has also been achieved by range-only distance sensors, such as acoustic beacons/transponders, [27–31]. As shown in Fig. 1(c), these sensors detect around 360° but provide no information on the directions of objects. Thus, rather than controlling their attitudes, the robots must move around to obtain the directions of other robots. Therefore, the formation control problem differs between proximity distance sensors and range-only distance sensors. Although the formation control problem has been investigated for range-only distance sensors well, it has not been for proximity distance sensors yet.

In the experiment, a leader-follower formation control is considered, where one leader is operated by a human while the others maintain the desired formation by the proposed method. The leader-follower formation is investigated by many papers, e.g. [32, 33]. The difference of the approach of this paper is that followers are equipped with only proximity distance sensors and can receive quite limited information on neighbors. We show that the formation can be maintained in this situation.

This paper uses the following notations. For a vector $x \in \mathbb{R}^2$, where $\mathbb{R}$ is the set of the real numbers, the Euclidean norm is described as $\|x\| = \sqrt{x^\top x}$. For non-zero vectors $x, y \in \mathbb{R}^2$, let $\angle(x,y) \in (-\pi, \pi]$ be the signed angle from x to y satisfying

$$\sin(\angle(x,y)) = \frac{\det([x\ y])}{\|x\|\|y\|},\ \cos(\angle(x,y)) = \frac{x^\top y}{\|x\|\|y\|},$$

where $\det(\cdot)$ is the determinant of a square matrix. Now, let $|\mathcal{N}|$ be the number of elements in a countable set $\mathcal{N}$. The rotation matrix of the angle $\theta \in (-\pi, \pi]$ is represented by the matrix function $R : (-\pi, \pi] \to SO(2)$ as

$$R(\theta) = \begin{bmatrix} \cos(\theta) & -\sin(\theta) \\ \sin(\theta) & \cos(\theta) \end{bmatrix}, \tag{1}$$

where $SO(2) \subset \mathbb{R}^{2\times 2}$ is the set of all two-by-two orthogonal matrices whose determinants are one. The unit vector at the angle $\theta \in (-\pi, \pi]$ from the x-axis on the plane is denoted by the vector function $e : (-\pi, \pi] \to S(1)$ as

$$e(\theta) = \begin{bmatrix} \cos(\theta) \\ \sin(\theta) \end{bmatrix}, \tag{2}$$

where $S(1) \subset \mathbb{R}^2$ is the set of all two-dimensional vectors whose norms are one.

The remainder of this paper is organized as follows. Section 2 gives the problem formulation of the formation control with proximity distance sensors. Section 3 presents the main result; namely, the design of the distributed motion controller. The experimental results and conclusions are given in Sections 4 and 5, respectively.

2. PROBLEM FORMULATION

2.1. System setting

Consider n omni-wheeled robots numbered from 1 to n in two-dimensional space. The set of the numbers is described as $\mathcal{V} = \{1, 2, \ldots, n\}$. All robots are considered are circles with with identical radius $r > 0$. The position of robot $i \in \mathcal{V}$ at time t is represented by the coordinate $x_i(t) \in \mathbb{R}^2$ in the the world coordinate system Σ. Let Σ_i be the relative coordinate system of robot i, where the origin is the center of robot i and the directions of the x- and y-axes are given by $e(\theta_i(t))$ and $e(\theta_i(t) + \pi/2)$ in Σ, respectively. Here, $\theta_i(t) \in (-\pi, \pi]$ represents the attitude angle of robot i in Σ. The geometry is shown in Fig. 2.

We assume that robot i can be controlled through its velocity and angular velocity in $\hat{\Sigma}_i$. The velocity and the

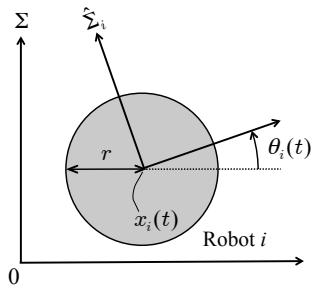

Fig. 2. Position coordinate $x_i(t)$ and attitude angle $\theta_i(t)$ in the world and relative coordinate systems Σ and $\hat{\Sigma}_i$.

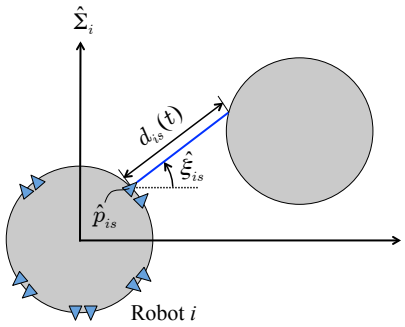

Fig. 3. Arrangement of proximity distance sensors.

angular velocity of robot i are then described in Σ by

$$\dot{x}_i(t) = R(\theta_i(t))\hat{v}_i(t), \tag{3}$$
$$\dot{\theta}_i(t) = \omega_i(t), \tag{4}$$

where $\hat{v}_i(t) \in \mathbb{R}^2$ and $\omega_i(t) \in \mathbb{R}$ are the velocity and the angular velocity inputs, respectively. Equations (3) and (4) represent the state equations of robot i in the state variables $x_i(t), \theta_i(t)$ under the control inputs $\hat{v}_i(t), \omega_i(t)$.

Each robot is equipped with multiple proximity distance sensors for detecting other robots. Let m_i be the number of sensors on robot i and let $\mathcal{S}_i = \{1, 2, \ldots, m_i\}$ be the set of these sensors. The arrangement of sensor $s \in \mathcal{S}_i$ is described by $(\hat{p}_{is}, \hat{\xi}_{is})$, where $\hat{p}_{is} \in \mathbb{R}^2$ is the position coordinate in $\hat{\Sigma}_i$ and $\hat{\xi}_{is} \in (-\pi, \pi]$ is the detection angle from the x-axis of $\hat{\Sigma}_i$. The situation is illustrated in Fig. 3. From sensor s, robot i obtains the distance $d_{is}(t) \geq 0$ to the surface of another robot. As illustrated in Fig. 3, one sensor can measure the distance from the side of a robot, not the center. Thus, the position of the center has to be estimated in some way by using several sensors.

The control input is then generated as

$$\hat{v}_i(t) = f_i(d_{i1}(t), d_{i2}(t), \ldots, d_{im_i}(t)), \tag{5}$$
$$\omega_i(t) = g_i(d_{i1}(t), d_{i2}(t), \ldots, d_{im_i}(t)), \tag{6}$$

where the functions $f_i : \mathbb{R}^{m_i} \to \mathbb{R}^2$ and $g_i : \mathbb{R}^{m_i} \to \mathbb{R}$ correspond to the position and attitude controllers, respectively.

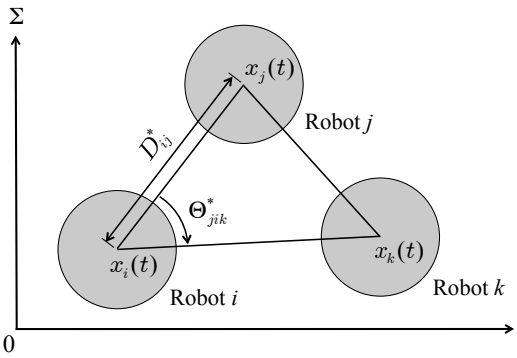

Fig. 4. Desired shape of the formation.

The controllers $\hat{v}_i(t)$ and $\omega_i(t)$ governed by (5) and (6), which are to be designed, are said to be *distributed over proximity distance sensors*. Note that the design includes not only the controllers, but also the number m_i of the sensors and the sensor arrangement $(\hat{p}_{is}, \hat{\xi}_{is})$.

2.2. Control objectives

The control objective is a specified formation of the robots. Let $\mathcal{N}_i \subset \mathcal{V}$ be the set of neighbors of robot $i \in \mathcal{V}$, with which desired distances and angles are assigned as follows: $D^*_{ij} > 2r$ is the desired distance between the centers of robots i and j; $\Theta^*_{jik} \in (-\pi, \pi]$ is the desired angle of the triangle with vertexes at the centers of robots i, j, and k as shown in Fig. 4. The control objectives are then formulated as

$$\lim_{t\to\infty} \|x_i(t) - x_j(t)\| = D^*_{ij}, \tag{7}$$
$$\lim_{t\to\infty} \angle(x_j(t) - x_i(t), x_k(t) - x_i(t)) = \Theta^*_{jik}. \tag{8}$$

Let $G = (\mathcal{V}, \mathcal{E})$ be the graph with the vertex set $\mathcal{V}$ and the edge set defined as $\mathcal{E} = \{(j,i) : j \in \mathcal{N}_i\}$. We assume that the graph G is *generically persistent* and that D^*_{ij} and Θ^*_{jik} for $j,k \in \mathcal{N}_i$ and $i \in \mathcal{V}$ are *realizable*. Roughly speaking, these assumptions dictate that if (7) and (8) are satisfied for all $j \in \mathcal{N}_i$ and $i \in \mathcal{V}$, the set of the coordinates $(x_1(t), x_2(t), \ldots, x_n(t))$ is uniquely determined but allows free rotation. These terminologies are furhter described in [34].

The main problem of this study is formulated as follows.

Problem 1: Given the set $\mathcal{N}_i \subset \mathcal{V}$ of neighbors, the desired distances $D^*_{ij} > 2r$, and the desired angles $\Theta^*_{jik} \in (-\pi, \pi]$ satisfying the above assumptions for $j,k \in \mathcal{N}_i$ and $i \in \mathcal{V}$, we assign the number m_i of the sensors and sensor arrangements $(\hat{p}_{is}, \hat{\xi}_{is})$ for all $s \in \mathcal{S}_i$, and design a control input $(\hat{v}_i(t), \omega_i(t))$ distributed over proximity distance sensors to achieve the control objectives (7) and (8). □

3. MAIN RESULT

3.1. Control objectives in the relative coordinate system

First, we describe the control objectives (7) and (8) in the relative coordinate system $\hat{\Sigma}_i$. Let $\hat{x}_{ij}(t) \in \mathbb{R}^2$ be the relative coordinate of robot j in $\hat{\Sigma}_i$. From Fig. 2, the relative coordinate $\hat{x}_{ij}(t)$ and absolute coordinates $x_i(t)$ and $x_j(t)$ are related by

$$x_j(t) - x_i(t) = R(\theta_i(t))\hat{x}_{ij}(t). \tag{9}$$

We now rewrite the control objectives (7) and (8) in terms of $\hat{x}_{ij}(t)$. Let $\hat{\theta}^*_{ij} \in (-\pi, \pi]$ ($j \in \mathcal{N}_i$) be a set of constants satisfying

$$\angle(e(\hat{\theta}^*_{ij}), e(\hat{\theta}^*_{ik})) = \Theta^*_{jik} \tag{10}$$

for all $j,k \in \mathcal{N}_i$. Then, (7) and (8) are obtained when the condition

$$\lim_{t\to\infty} \hat{x}_{ij}(t) = D^*_{ij} e(\hat{\theta}^*_{ij}) \tag{11}$$

holds for all $j \in \mathcal{N}_i$. Formally, we can write the following theorem.

Theorem 1: Given constants $\hat{\theta}^*_{ij} \in (-\pi, \pi]$ satisfying (10) for any $j,k \in \mathcal{N}_i$, objectives (7) and (8) are achieved if (11) holds for all $j,k \in \mathcal{N}_i$.

Proof: First, from (9) and (11), we obtain

$$\begin{aligned}\lim_{t\to\infty} \|x_i(t) - x_j(t)\| &= \lim_{t\to\infty} \|R(\theta_i(t))\hat{x}_{ij}(t)\| \\ &= \lim_{t\to\infty} \|\hat{x}_{ij}(t)\| = \|D^*_{ij} e(\hat{\theta}^*_{ij})\| \\ &= D^*_{ij},\end{aligned}$$

which achieves objective (7). Next, from (9), (10), and (11), we have

$$\begin{aligned}&\lim_{t\to\infty} \angle(x_j(t) - x_i(t), x_k(t) - x_i(t)) \\ &= \lim_{t\to\infty} \angle(\hat{x}_{ij}(t), \hat{x}_{ik}(t)) = \angle(e(\hat{\theta}^*_{ij}), e(\hat{\theta}^*_{ik})) \\ &= \Theta^*_{jik},\end{aligned}$$

which achieves objective (8). □

Theorem 1 successfully divides our task for solving Problem 1 into two parts: designing the control inputs $\hat{v}_i(t), \omega_i(t)$ for (11) and assigning the sensor arrangement $(\hat{p}_{is}, \hat{\xi}_{is})$ for (10). These solutions are discussed in the following subsections.

3.2. Design of controllers based on relative coordinates

We say that the controllers $\hat{v}_i(t)$ and $\omega_i(t)$ are *distributed* in the relative coordinate system $\hat{\Sigma}_i$ if they are generated as

$$\hat{v}_i(t) = \hat{f}_i(\hat{x}_{ij_1}(t), \hat{x}_{ij_2}(t), \ldots, \hat{x}_{ij_{|\mathcal{N}_i|}}(t)), \tag{12}$$

$$\omega_i(t) = \hat{g}_i(\hat{x}_{ij_1}(t), \hat{x}_{ij_2}(t), \ldots, \hat{x}_{ij_{|\mathcal{N}_i|}}(t)), \tag{13}$$

where the functions $\hat{f}_i : \mathbb{R}^{2|\mathcal{N}_i|} \to \mathbb{R}^2$, $\hat{g}_i : \mathbb{R}^{2|\mathcal{N}_i|} \to \mathbb{R}$, and $\{j_1, j_2, \ldots, j_{|\mathcal{N}_i|}\} = \mathcal{N}_i$. Here, we design the controllers distributed in $\hat{\Sigma}_i$ to satisfy (11). Based on this design, controllers distributed over proximity distance sensors are designed in the next subsection.

Now, consider the optimization problem

$$\underset{x_i \in \mathbb{R}^2, \theta_i \in (-\pi,\pi]}{\text{minimize}} \quad V_i(x_i, \theta_i) \tag{14}$$

with the objective function

$$V_i(x_i, \theta_i) = \frac{1}{2} \sum_{j \in \mathcal{N}_i} \left\| R^\top(\theta_i)(x_j - x_i) - D^*_{ij} e(\hat{\theta}^*_{ij}) \right\|^2, \tag{15}$$

which represents the difference between the left- and right-hand sides of (11) for all $j \in \mathcal{N}_i$, where we have used relation (9).

To satisfy condition (11), the control of robot i needs only to decrease $V_i(x_i(t), \theta_i(t))$. This is realized by the following gradient-based controllers:

$$\hat{v}_i(t) = -k_{x_i} R^\top(\theta_i(t)) \frac{\partial V_i}{\partial x_i}(x_i(t), \theta_i(t)), \tag{16}$$

$$\omega_i(t) = -k_{\theta_i} \frac{\partial V_i}{\partial \theta_i}(x_i(t), \theta_i(t)) \tag{17}$$

for $k_{x_i}, k_{\theta_i} > 0$. Actually, from (3), (4), (16), and (17), we obtain

$$\begin{aligned}\dot{V}_i(t) =& \frac{\partial V_i}{\partial x_i}(x_i(t), \theta_i(t))\dot{x}_i(t) + \frac{\partial V_i}{\partial \theta_i}(x_i(t), \theta_i(t))\dot{\theta}_i(t) \\ =& -k_{x_i} \left\| \frac{\partial V_i}{\partial x_i}(x_i(t), \theta_i(t)) \right\|^2 \\ & - k_{\theta_i} \left\| \frac{\partial V_i}{\partial \theta_i}(x_i(t), \theta_i(t)) \right\|^2 \le 0,\end{aligned} \tag{18}$$

whereby $V_i(t)$ is monotonically decreasing and $\lim_{t\to\infty} V_i(t) = 0$ is (locally) obtained. Condition (11) then follows from (15).

We now show that the gradient-based controllers given by (16) and (17) are distributed in the relative coordinate system $\hat{\Sigma}_i$.

Theorem 2: The controllers

$$\hat{v}_i(t) = k_{x_i} \sum_{j \in \mathcal{N}_i} \left(\hat{x}_{ij}(t) - D^*_{ij} e(\hat{\theta}^*_{ij}) \right), \tag{19}$$

$$\omega_i(t) = k_{\theta_i} \sum_{j \in \mathcal{N}_i} D^*_{ij} \hat{x}^\top_{ij}(t) e(\hat{\theta}^*_{ij} + \pi/2) \tag{20}$$

are distributed in the relative coordinate system $\hat{\Sigma}_i$, and are equivalent to the gradient-based controllers (16) and (17) for $V_i(x_i, \theta_i)$ in (15).

Proof: First, (19) and (20) are of the forms (12) and (13), respectively. Thus, they are distributed in the relative coordinate system $\hat{\Sigma}_i$.

Next, (15) reduces to

$$V_i(x_i,\theta_i)=\sum_{j\in\mathcal{N}_i}\left(\frac{1}{2}(x_j-x_i)^\top(x_j-x_i)+\frac{{D^*_{ij}}^2}{2}-D^*_{ij}(x_j-x_i)^\top R(\theta_i)e(\hat{\theta}^*_{ij})\right). \quad (21)$$

The partial derivative of (21) with respect to x_i is calculated as

$$\begin{aligned}\frac{\partial V_i}{\partial x_i}(x_i,\theta_i)&=-\sum_{j\in\mathcal{N}_i}\left((x_j-x_i)-D^*_{ij}R(\theta_i)e(\hat{\theta}^*_{ij})\right)\\&=-\sum_{j\in\mathcal{N}_i}\left(R(\theta_i)\hat{x}_{ij}-D^*_{ij}R(\theta_i)e(\hat{\theta}^*_{ij})\right), \quad (22)\end{aligned}$$

where $\hat{x}_{ij}=R^\top(\theta_i)(x_j-x_i)$. Then, (16) and (22) lead to (19). The partial derivative of (21) with respect to θ_i is calculated as

$$\begin{aligned}\frac{\partial V_i}{\partial \theta_i}(x_i,\theta_i)&=-\sum_{j\in\mathcal{N}_i}D^*_{ij}(x_j-x_i)^\top\frac{\partial R(\theta_i)}{\partial\theta_i}e(\hat{\theta}^*_{ij})\\&=-\sum_{j\in\mathcal{N}_i}D^*_{ij}\hat{x}_{ij}^\top R^\top(\theta_i)\begin{bmatrix}-\sin(\theta_i)&-\cos(\theta_i)\\\cos(\theta_i)&-\sin(\theta_i)\end{bmatrix}e(\hat{\theta}^*_{ij})\\&=-\sum_{j\in\mathcal{N}_i}D^*_{ij}\hat{x}_{ij}^\top\begin{bmatrix}0&-1\\1&0\end{bmatrix}e(\hat{\theta}^*_{ij})\\&=-\sum_{j\in\mathcal{N}_i}D^*_{ij}\hat{x}_{ij}^\top R(\pi/2)e(\hat{\theta}^*_{ij}). \quad (23)\end{aligned}$$

Then, (17) and (23) lead to (20). □

Remark 1: The optimization function (15) is non-convex, and thus the global attraction is not guaranteed from (18). Therefore, the initial coordination of the robots has to be close to the desired formation. This issue is common in the research on control of multiple robots, e.g. formation control [12, 14] and coverage control [35]. Thus, a strategy to overcome this difficult is demanded in this discipline, which is important future work. □

3.3. Design of controllers distributed over proximity distance sensors

In this subsection, we transform the designed controllers (19) and (20) into controllers distributed over proximity distance sensors.

To this end, we first derive the relative coordinate $\hat{x}_{ij}(t)$ of the center of robot j in $\hat{\Sigma}_i$ from the measured values of the proximity distance sensors. Let $\hat{q}_{ij}(t)\in\mathbb{R}^2$ be the coordinate on the surface of robot j with angle $\hat{\theta}^*_{ij}$ from the x-axis of $\hat{\Sigma}_i$ as illustrated in Fig. 5. If more than one point satisfies this condition, the nearest point to the origin is selected. This coordinate is then defined as

$$\hat{q}_{ij}(t)=\ell_{ij}(t)e(\hat{\theta}^*_{ij}), \quad (24)$$

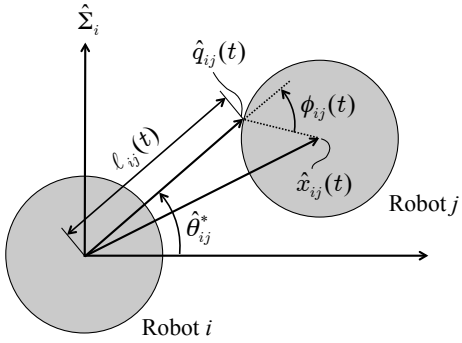

Fig. 5. Coordinate on the surface of the robot.

where $\ell_{ij}(t)>0$ is the norm of $\hat{q}_{ij}(t)$, described as

$$\ell_{ij}(t)=\min\{\ell>0:\|\ell e(\hat{\theta}^*_{ij})-\hat{x}_{ij}(t)\|=r\}. \quad (25)$$

From (24) and (25), we have

$$\|\hat{x}_{ij}(t)-\hat{q}_{ij}(t)\|=r. \quad (26)$$

Let $\phi_{ij}(t)\in(-\pi,\pi]$ be the angle from $\hat{x}_{ij}(t)-\hat{q}_{ij}(t)$ to $\hat{q}_{ij}(t)$ as

$$\phi_{ij}(t)=\angle(\hat{x}_{ij}(t)-\hat{q}_{ij}(t),\hat{q}_{ij}(t)). \quad (27)$$

Then, from (24), (26), and (27), we obtain

$$\hat{x}_{ij}(t)-\hat{q}_{ij}(t)=re(\hat{\theta}^*_{ij}-\phi_{ij}(t)). \quad (28)$$

From (24) and (28), $\hat{x}_{ij}(t)$ is described as

$$\begin{aligned}\hat{x}_{ij}(t)&=\hat{q}_{ij}(t)+(\hat{x}_{ij}(t)-\hat{q}_{ij}(t))\\&=\ell_{ij}(t)e(\hat{\theta}^*_{ij})+re(\hat{\theta}^*_{ij}-\phi_{ij}(t)). \quad (29)\end{aligned}$$

If proximity distance sensors are appropriately arranged, $\hat{x}_{ij}(t)$ can be estimated by the sensors through (29). By comparing (5) and (12) (or (6) and (13)), we infer that robot i requires at least $2|\mathcal{N}_i|$ sensors. We thus assign $m_i=2|\mathcal{N}_i|$ sensors to each robot and let each sensor pair detect a different robot. Now let $s^+_{ij},s^-_{ij}\in\mathcal{S}_i$ be the pair of the sensors that detect robot j and arrange these sensors such that

$$\hat{p}_{is^+_{ij}}=re(\hat{\theta}^*_{ij}+\delta_{ij}),\ \hat{p}_{is^-_{ij}}=re(\hat{\theta}^*_{ij}-\delta_{ij}), \quad (30)$$

$$\hat{\xi}_{is^+_{ij}}=\hat{\theta}^*_{ij},\ \hat{\xi}_{is^-_{ij}}=\hat{\theta}^*_{ij} \quad (31)$$

for some $\delta_{ij}>0$ as presented in Fig. 6. Equation (30) means that the sensors are located at the edge of robot i around the angle $\hat{\theta}^*_{ij}$ in $\hat{\Sigma}_i$ with an interval of $2\delta_{ij}$. Equation (31) means that both the detection angles are $\hat{\theta}^*_{ij}$ in $\hat{\Sigma}_i$. Note that distances $d_{is^+_{ij}}(t)$ and $d_{is^-_{ij}}(t)$ measured by sensors s^+_{ij} and s^-_{ij} depend on δ_{ij}, thus we define the two variables

$$\bar{d}_{ij}(t,\delta_{ij})=\frac{d_{is^+_{ij}}(t)+d_{is^-_{ij}}(t)}{2}, \quad (32)$$

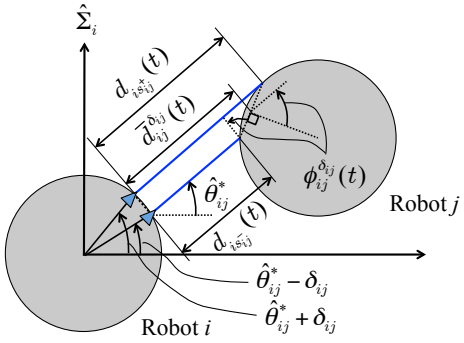

Fig. 6. Sensor arrangement.

$$\phi_{ij}(t,\delta_{ij}) = \tan^{-1}\left(\frac{d_{is_{ij}^+}(t) - d_{is_{ij}^-}(t)}{r\sin(2\delta_{ij})}\right). \tag{33}$$

From Fig. 6, we find that

$$\lim_{\delta_{ij}\to+0} \bar{d}_{ij}(t,\delta_{ij}) = \ell_{ij}(t) - r, \tag{34}$$

$$\lim_{\delta_{ij}\to+0} \phi_{ij}(t,\delta_{ij}) = \phi_{ij}(t) \tag{35}$$

are satisfied. Equations (32), (33), (34), and (35) imply that for sufficiently small δ_{ij}, the values of $\ell_{ij}(t)$ and $\phi_{ij}(t)$ can be estimated from the measured values $d_{is_{ij}^+}(t)$ and $d_{is_{ij}^-}(t)$. The relative coordinate $\hat{x}_{ij}(t)$ is then estimated from (29).

From the above discussion, we obtain the following theorem.

Theorem 3: For the two variables

$$\begin{aligned}
&\hat{v}_i(t,\delta_{ij}) \\
&= k_{x_i}\sum_{j\in\mathcal{N}_i}\left(\left(\frac{d_{is_{ij}^+}(t) + d_{is_{ij}^-}(t)}{2} + r - D_{ij}^*\right)e(\hat{\theta}_{ij}^*)\right. \\
&\quad \left. + re\left(\hat{\theta}_{ij}^* - \tan^{-1}\left(\frac{d_{is_{ij}^+}(t) - d_{is_{ij}^-}(t)}{r\sin(2\delta_{ij})}\right)\right)\right),
\end{aligned} \tag{36}$$

$$\begin{aligned}
&\omega_i(t,\delta_{ij}) \\
&= k_{\theta_i}\sum_{j\in\mathcal{N}_i}\frac{-rD_{ij}^*(d_{is_{ij}^+}(t) - d_{is_{ij}^-}(t))}{\sqrt{(d_{is_{ij}^+}(t) - d_{is_{ij}^-}(t))^2 + (r\sin(2\delta_{ij}))^2}},
\end{aligned} \tag{37}$$

the controllers $\hat{v}_i(t) = \hat{v}_i(t,\delta_{ij})$ and $\omega_i(t) = \omega_i(t,\delta_{ij})$ are distributed over proximity distance sensors. Moreover, $\lim_{\delta_{ij}\to+0}\hat{v}_i(t,\delta_{ij})$ and $\lim_{\delta_{ij}\to+0}\omega_i(t,\delta_{ij})$ are gradient-based controllers of $V_i(x_i,\theta_i)$ in (15).

Proof: Equations (36) and (37) are explicit forms of (5) and (6), respectively, from $s_{ij}^+, s_{ij}^- \in \mathcal{S}_i = \{1,2,\ldots,m_i\}$. We then find that $\hat{v}_i(t) = \hat{v}_i(t,\delta_{ij})$ and $\omega_i(t) = \omega_i(t,\delta_{ij})$ are distributed over proximity distance sensors.

Next, inserting (32) and (33) in (36), we get

$$\begin{aligned}
\hat{v}_i(t,\delta_{ij}) =& k_{x_i}\sum_{j\in\mathcal{N}_i}\left((\bar{d}_{ij}(t,\delta_{ij}) + r)e(\hat{\theta}_{ij}^*)\right. \\
&\left. + re(\hat{\theta}_{ij}^* - \phi_{ij}(t,\delta_{ij})) - D_{ij}^* e(\hat{\theta}_{ij}^*)\right) \\
=& k_{x_i}\sum_{j\in\mathcal{N}_i}\left(\hat{x}_{ij}(t,\delta_{ij}) - D_{ij}^* e(\hat{\theta}_{ij}^*)\right),
\end{aligned} \tag{38}$$

where

$$\hat{x}_{ij}(t,\delta_{ij}) = (\bar{d}_{ij}(t,\delta_{ij}) + r)e(\hat{\theta}_{ij}^*) + re(\hat{\theta}_{ij}^* - \phi_{ij}(t,\delta_{ij})).$$

From (29), (34), and (35), we obtain

$$\lim_{\delta_{ij}\to+0}\hat{x}_{ij}(t,\delta_{ij}) = \hat{x}_{ij}(t) \tag{39}$$

and from (38) and (39), $\lim_{\delta_{ij}\to+0}\hat{v}_i(t,\delta_{ij})$ reduces to the right-hand side of (19). Next, from (33) and the relation $\sin(\tan^{-1}(a)) = a/\sqrt{a^2+1}$ for $a\in\mathbb{R}$, (37) reduces to

$$\omega_i(t,\delta_{ij}) = -k_{\theta_i} r\sum_{j\in\mathcal{N}_i} D_{ij}^*\sin(\phi_{ij}(t,\delta_{ij})). \tag{40}$$

On the other hand, from (29), (20) reduces to

$$\begin{aligned}
\omega_i(t) =& k_{\theta_i}\sum_{j\in\mathcal{N}_i} D_{ij}^*(\ell_{ij}(t)e(\hat{\theta}_{ij}^*) + re(\hat{\theta}_{ij}^* - \phi_{ij}(t)))^\top \\
&\times e(\hat{\theta}_{ij}^* + \pi/2) \\
=& k_{\theta_i} r\sum_{j\in\mathcal{N}_i} D_{ij}^* e^\top(\hat{\theta}_{ij}^* - \phi_{ij}(t))e(\hat{\theta}_{ij}^* + \pi/2) \\
=& k_{\theta_i} r\sum_{j\in\mathcal{N}_i} D_{ij}^*\cos(\pi/2 + \phi_{ij}(t)) \\
=& -k_{\theta_i} r\sum_{j\in\mathcal{N}_i} D_{ij}^*\sin(\phi_{ij}(t)).
\end{aligned} \tag{41}$$

From (35), (40), and (41), $\lim_{\delta_{ij}\to+0}\omega_i(t,\delta_{ij})$ reduces to the right-hand side of (20). Therefore, Theorem 2 guarantees that $\lim_{\delta_{ij}\to+0}\hat{v}_i(t,\delta_{ij})$ and $\lim_{\delta_{ij}\to+0}\omega_i(t,\delta_{ij})$ are equivalent to the gradient-based controllers (16) and (17), respectively, of $V_i(x_i,\theta_i)$ in (15). □

Consequently, the proposed position and attitude controllers are given by (36) and (37), respectively, which do not depend on the global coordinate, but depend on only the local information from the proximity distance sensors. From this viewpoint, these controllers are distributed over proximity distance sensors. Even in this situation, the control objectives (7), (8) are achievable because they are based on the relative distances $\|x_i(t) - x_j(t)\|$ and angles $\angle(x_j(t) - x_i(t), x_k(t) - x_i(t))$ between the robots, which are independent of the global coordinate.

3.4. Implementation procedure

For the set $\mathcal{N}_i \subset \mathcal{V}$ of neighbors, the desired distances $D_{ij}^* > 2r$, and the desired angles $\Theta_{jik}^* \in (-\pi,\pi]$ where $j,k\in\mathcal{N}_i$ and $i\in\mathcal{V}$, we can implement the formation control according to the following procedure.

1) Assign $m_i = 2|\mathcal{N}_i|$ proximity distance sensors to each robot.
2) Choose numbers $\hat{\theta}_{ij}^* \in (-\pi,\pi]$ for $j\in\mathcal{N}_i$ satisfying (10) from Θ_{jik}^*.

3) Mount the sensors at the coordinates (30) and the detection angles (31) in $\hat{\Sigma}_i$ for some $\delta_{ij} > 0$.

4) Implement the controllers $\hat{v}_i(t) = \hat{v}_i(t, \delta_{ij})$ and $\omega_i(t) = \omega_i(t, \delta_{ij})$ given in (36) and (37) with some gains $k_{x_i} > 0$ and $k_{\theta_i} > 0$.

Theorem 3 guarantees that the controllers are distributed over proximity distance sensors and approximate the gradient of $V_i(x_i, \theta_i)$ in (15). Therefore, $V_i(t)$ will decrease according to (18), and $\lim_{t\to\infty} V_i(t) = 0$ is achieved. Condition (11) is then locally obtained from (15). Finally, control objectives (7) and (8) are guaranteed by Theorem 1.

When we choose the value of δ_{ij} in (c), we need to consider a trade-off between the estimation accuracy and the noise robustness, which is explained as follows. Equations (34) and (35) indicate that the smaller δ_{ij} is, the more accurately the length $\ell_{ij}(t) - r$ and the angle $\phi_{ij}(t)$ are estimated. This is true without noise in sensor signals. In contrast, noise makes the estimation worse as δ_{ij} is smaller. Therefore, we need to choose appropriate δ_{ij} according to the noise level. Such a method should be developed in future work.

When we choose the gains k_{x_i}, k_{θ_i} in (d), the balance between the gains plays a key role to achieve natural robot motions, which can be seen from the differential of $V_i(x_i, \theta_i)$ in (18) as follows. Let $\varepsilon_{ij}(t) \in \mathbb{R}^2$ be the error of $\hat{x}_{ij}(t) \in \mathbb{R}^2$ from the desired position $D^*_{ij} e(\hat{\theta}^*_{ij})$, namely $\hat{x}_{ij}(t) = D^*_{ij} e(\hat{\theta}^*_{ij}) + \varepsilon_{ij}(t)$. Assume that the neighbor set consists of one robot, namely $\mathcal{N}_i = \{j\}$. Then, from (22) and (23), the following two are obtained:

$$\left\| \frac{\partial V_i}{\partial x_i}(x_i(t), \theta_i(t)) \right\| = \|\varepsilon_{ij}(t)\|,$$
$$\left\| \frac{\partial V_i}{\partial \theta_i}(x_i(t), \theta_i(t)) \right\| = D^*_{ij} \|\varepsilon^\top_{ij}(t) e(\hat{\theta}^*_{ij})\| \le D^*_{ij} \|\varepsilon_{ij}(t)\|.$$

Then, from (18), we can estimate the value of $\dot{V}_i(t)$ as

$$\dot{V}_i(t) \ge -k_{x_i} \|\varepsilon_{ij}(t)\|^2 - k_{\theta_i} (D^*_{ij})^2 \|\varepsilon_{ij}(t)\|^2, \tag{42}$$

where the two terms of the right-hand side represent the effects to $V_i(x_i, \theta_i)$ from the position control and the attitude control, respectively. Then, (42) shows that k_{x_i} should approximate to $k_{\theta_i} (D^*_{ij})^2$ to balance these two control effects for natural robot motions.

Remark 2: We do not consider the situation that $\mathcal{N}_i$ is time-varying because the proposed attitude controller (20) (or (37)) works so as to keep $\mathcal{N}_i$ invariant. However, $\mathcal{N}_i$ possibly varies in practical situations. The extension to the time-varying case is not straightforward because the objective function (15) varies discontinuously when $\mathcal{N}_i$ changes. The time-varying case is important future work. □

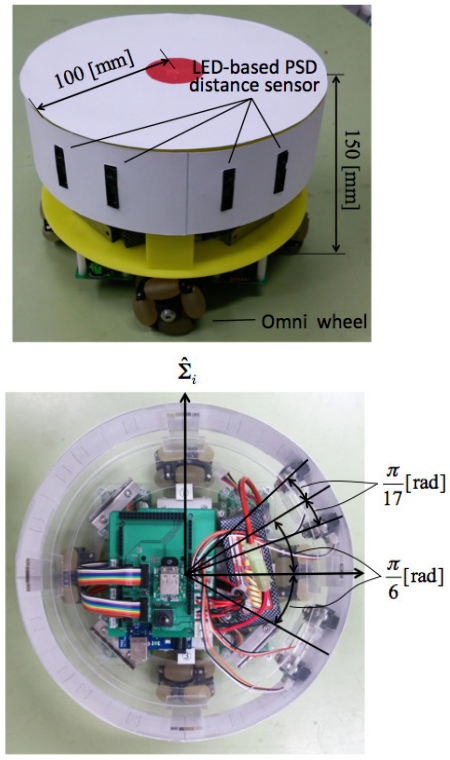

Fig. 7. Exterior and interior of the omni-wheeled robot used in the experiment.

4. EXPERIMENT

This section demonstrates the effectiveness of the proposed method through an experiment on six($= n$) identical omni-wheeled robots. The robotic group consists of one leader and five follows. The leader is controlled by a human operator while each follower follows the leader or other followers.

All the followers are uniform, whose exterior and interior are photographed in Fig. 7. The robots are cylindrical with radius $r = 100$ mm. Each robot is 150 mm high and weighs 1.68 kg. The robots are moved by stepping motors (SM-42BYG011-25) operated through motor drivers (L6470), and are equipped with one-board computers (Arduino Mega 2560) and LED-based PSD proximity distance sensors (GP2Y0A21YK0F). Because of the uniformity of the followers, we can easily enlarge the scale of the robotic group just by adding the uniform type of robots.

The desired formation is shown in Fig. 8, where the arrows point to the neighbors. This formation is chosen for the uniform followers shown in Fig. 7. Actually, each of the followers (Robots $2 \sim 6$) has two neighbors corresponding to two pairs of the sensors. The neighbor set $\mathcal{N}_i$ of each robot is then given as follows:

$$\mathcal{N}_1 = \emptyset, \mathcal{N}_2 = \{1, 3\}, \mathcal{N}_3 = \{1, 2\},$$

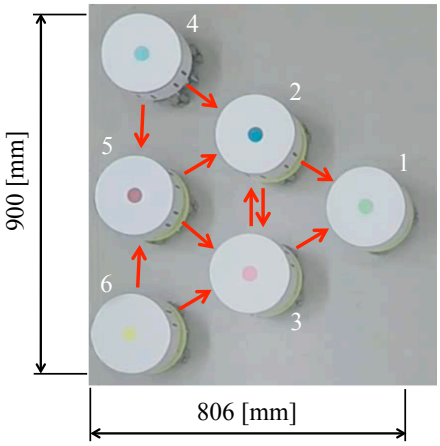

Fig. 8. Desired formation in the experiment.

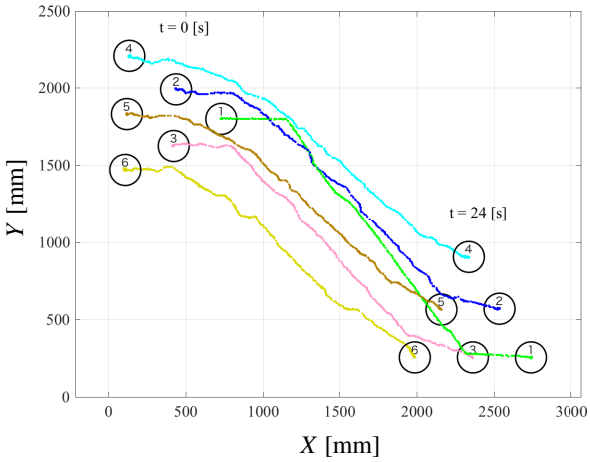

Fig. 9. Trajectories of the coordinates of the robots in the experiment.

$$\mathcal{N}_4 = \{2,5\},\ \mathcal{N}_5 = \{2,3\},\ \mathcal{N}_6 = \{3,5\}, \tag{43}$$

where $\emptyset$ represents the empty set. The desired distances between any robot pair i and $j \in \mathcal{N}_i$ was $D^*_{ij} = 350$ mm. The desired angles were given as

$$\Theta^*_{321} = \Theta^*_{132} = \Theta^*_{542} = \Theta^*_{352} = \Theta^*_{365} = \frac{\pi}{3} \text{ rad}. \tag{44}$$

We now arrange the distance sensors and design controllers as described in Subsection 3.4

1) From (43), assign the number of sensors of each robot as $m_1 = 0$, $m_2 = m_3 = m_4 = m_5 = m_6 = 4$.
2) From (44), select $\hat{\theta}^*_{ij}$ to satisfy (10) as

$$\hat{\theta}^*_{23} = \hat{\theta}^*_{31} = \hat{\theta}^*_{45} = \hat{\theta}^*_{53} = \hat{\theta}^*_{63} = -\frac{\pi}{6} \text{ rad},$$
$$\hat{\theta}^*_{21} = \hat{\theta}^*_{32} = \hat{\theta}^*_{42} = \hat{\theta}^*_{52} = \hat{\theta}^*_{65} = \frac{\pi}{6} \text{ rad}.$$

3) Mount the sensors at the position coordinates (30) with detection angles (31) for $\delta_{ij} = \pi/17$ rad as shown in Fig. 7.
4) Implement the controllers (36) and (37) on the one-board computer, setting the gains $k_{x_i} = 165$ and $k_{\theta_i} = 0.002$. These gains are chosen according to the policy on the third paragraph of Subsection 3.4 Actually, the value of $k_{\theta_i}(D^*_{ij})^2 = 0.002 \times 350^2 = 245$ is similar to $k_{x_i} = 165$.

The experimental robot trajectories and snapshots of the robot formation are shown in Figs. 9 and 10, respectively. In this experiment, Robot 1 was controlled by human operation. Although Robot 1 changed the direction at two time points ($t = 6$ sec and $t = 18$ sec), Robots 2-6 maintained the desired formation in Fig. 8 and successfully followed Robot 1 (See Fig. 10).

Fig. 11 shows the time-transitions of the X- and Y-coordinates of the robots. The upper figure of Fig. 12

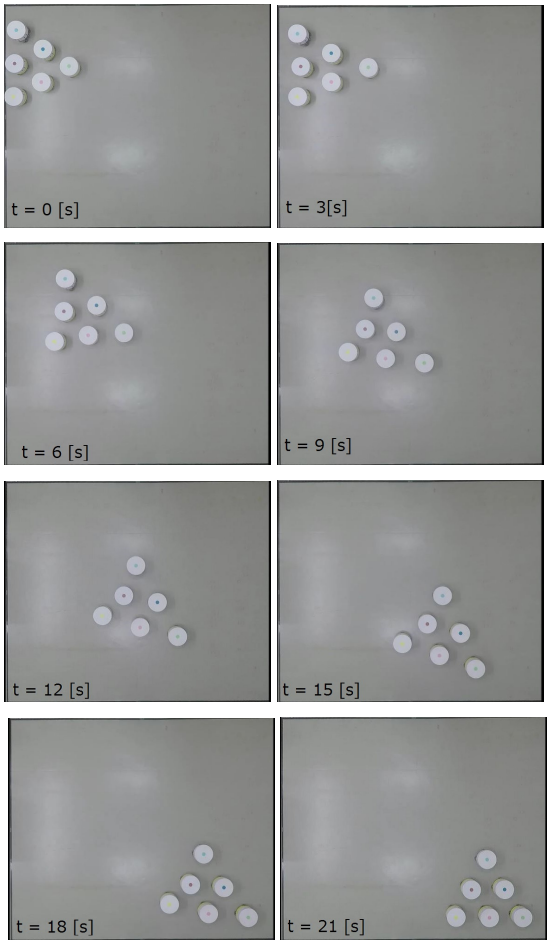

Fig. 10. Successive photographs captured during the experiment.

shows the time-transitions of the distances $\|x_i(t) - x_j(t)\|$ between the robots $(i,j) = (1,2)$, $(1,3)$, $(2,3)$, $(2,4)$, $(2,5)$, $(3,5)$, $(3,6)$, $(4,5)$, $(5,6)$ and the desired dis-

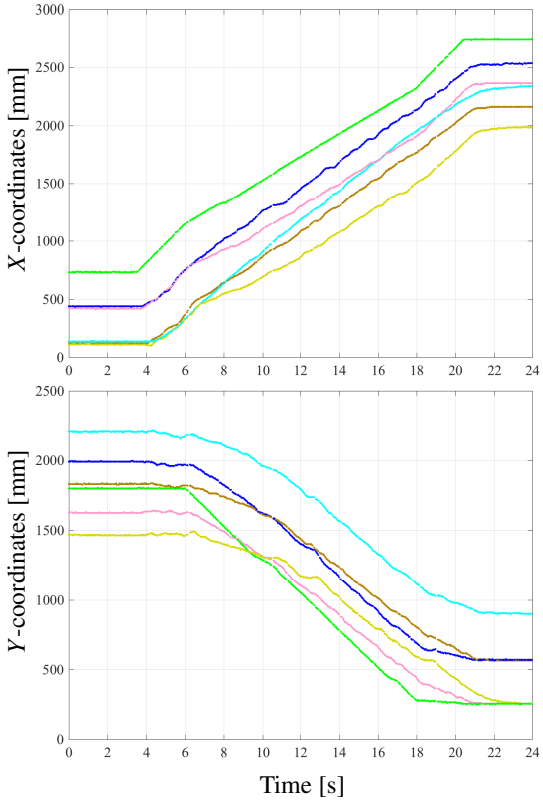

Fig. 11. Time-transitions of the X-, Y-coordinates of the robots in the experiment.

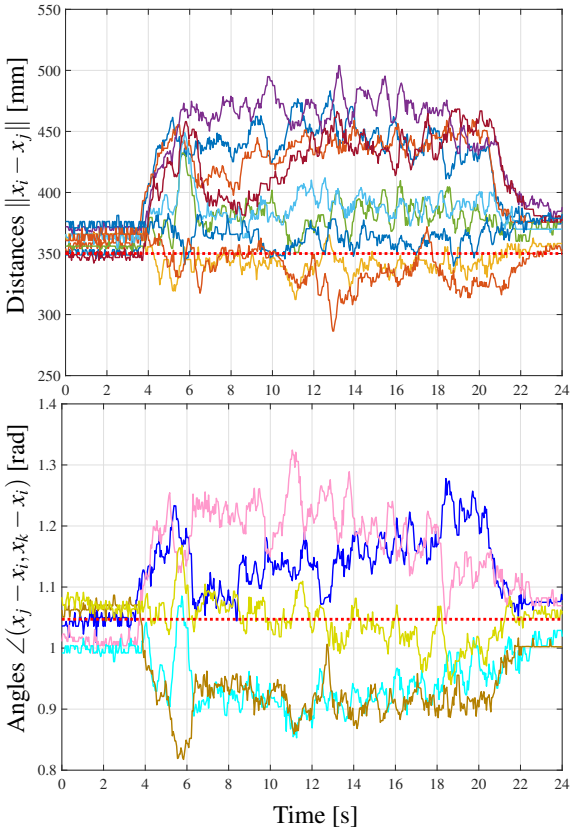

Fig. 12. Time-transitions of the distances $\|x_i - x_j\|$, angles $\angle(x_j - x_i, x_k - x_i)$ in the experiment with the desired values D^*_{ij}, Θ^*_{jik} in the red dotted lines.

tances $D^*_{ij} = 350$ [mm] in the red dotted line. The lower one shows the time-transitions of the angles $\angle(x_j(t) - x_i(t), x_k(t) - x_i(t))$ between the robots $(j,i,k) = (3,2,1)$, $(1,3,2)$, $(5,4,2)$, $(3,5,2)$, $(3,6,5)$ and the desired angles $\Theta^*_{jik} = \pi/3$ [rad] in the red dotted line. It is observed that the distances and angles track the desired values with some errors, and the control objectives (7), (8) are almost fulfilled.

The experimental result shows the robustness of the proposed method to the leader's operation because the formation is reasonably maintained even when the leader moves unexpectedly. Nevertheless, there remains a slight formation error since the followers are not informed of the trajectory or velocity of the leader and the leader's motion works as noise to the followers.

5. CONCLUSION

This study investigated the formation control problem of swarm robots using position sensitive detector (PSD) proximity distance sensors based on light-emitting diodes (LEDs). Using the gradient-based approach, we designed a motion controller with two parts: a position and an attitude controller. The attitude controller solves the inherent difficulty in proximity distance sensors; that is, the continuous detection of other robots through the narrow detection angles. We also achieved an appropriate sensor arrangement (positions and detection angles) that maintained the desired formation pattern. The proposed method was validated in an experiment performed by six omni-wheeled robots equipped with LED-based PSD proximity distance sensors.

When a robot detects no other robots, the present controllers do not work well. In such a situation, we need a different strategy to detect other robots beyond the range of the proximity distance sensors, e.g., installing the same type of proximity distance sensor redundantly. Then, the robot can continuously detect other robots with some of the sensors. Even though the robots are equipped with redundant sensors, the sensor system is still simpler than wide-directional sensors such as cameras and laser rangefinders. Then, the different problem arises: how to deal with the redundant information, which is important future work.

APPENDIX A

A.1. Comparison of distance sensors

In this section, we compare the detection ranges of (a) proximity distance sensors, (b) wide-angle distance

sensors, and (c) range-only distance sensors, which are shown in Fig. 1. Because of the difference of the detection ranges, we need different methods to estimate other robots' locations.

First, from (b) wide-angle distance sensors, the information on the distance $d(\xi) > 0$ is available as a function depending on the direction angle $\xi \in [-\xi_l, \xi_u)$, where $\xi_l, \xi_u \in [-\pi, \pi]$ is the lower and upper limits of the sensing range. We assume that ξ_l, ξ_u are close to $-\pi, \pi$, respectively, and the robot can achieve full information on its surroundings.

Second, from (a) proximity distance sensors, the information on the distances $d_s > 0$ from sensors $s = 1, 2, \ldots, m$ is available. Let $\hat{\xi}_s \in [-\pi, \pi)$ be the mounting angle of sensor $s \in \{1, 2, \ldots, m\}$. Then, the correspondence between (a) and (b) is described as $d_s = d(\hat{\xi}_s)$, which indicates that the available information by (a) is discretized from (b). Thus, (a) provides much less information than (b), and needs an advanced technique to estimate other robots' locations as developed in this paper.

Finally, from (c) range-only distance sensors, the information on distance $d_s > 0$ from sensors $s = 1, 2, \ldots, m$ is also available. However, each signal from (c) is independent of the mounting angle, and does not provide information on the directions of other robots differently from (a). Therefore, (c) gives less information than (a). Other robots' locations can be estimated from the time-transitions of d_s and/or the differences in received signals' phases. Note that (c) does not require attitude control because the signals can be received regardless of the robot attitude while (a) needs it due to the small detection angles. From this viewpoint, (a) imposes an additional control task on the formation control problem.

REFERENCES

[1] V. Kumar, D. Rus, and S. Singh, "Robot and sensor networks for first responders," *IEEE Pervasive Comput.*, vol. 3, no. 4, pp. 24-33, Oct.-Dec. 2004. [click]

[2] J. G. Bellingham and K. Rajan, "Robotics in remote and hostile environments," *Science*, vol. 318, no. 5853, pp. 1098-1102, Nov. 2007. [click]

[3] G. Sukhatme, A. Dhariwal, B. Zhang, C. Oberg, B. Stauffer, and D. Caron, "Design and development of a wireless robotic networked aquatic microbial observing system," *Environmental Engineering Science*, vol. 24, no. 2, pp. 205-215, Feb. 2007. [click]

[4] R. R. Murphy, J. Kravitz, S. L. Stover, and R. Shoureshi, "Mobile robots in mine rescue and recovery," *IEEE Robot. Autom. Mag.*, vol. 16, no. 2, pp. 91-103, Jun. 2009.

[5] G. Hattenberger, R. Alami, and S. Lacroix, "Planning and control for unmanned air vehicle formation flight," *Proc. of the 2006 IEEE/RSJ Int. Conf. on Intelligent Robots and Systems*, 2006.

[6] I. Maza, F. Caballero, J. Capitán, J. R. M. de Dios, and A. Ollero, "Experimental results in multi-UAV coordination for disaster management and civil security applications," *Journal of Intelligent & Robotic Systems*, vol. 61, no. 1, pp. 563-585, Jan. 2011. [click]

[7] E. Fiorelli, N. E. Leonard, P. Bhatta, and D. Paley, "Multi-AUV control and adaptive sampling in monterey bay," *Proc. of the IEEE Autonomous Underwater Vehicles 2004: Workshop on Multiple AUV Operations*, 2004.

[8] H. Yang and F. Zhang, "Geometric formation control for autonomous underwater vehicles," *Proc. of the 2010 IEEE Int. Conf. on Robotics and Automation*, 2010.

[9] H. Laakso, M. Taylor, and C. P. Escoubet, Eds., *The Cluster Active Archive: Studying the Earth's Space Plasma Environment*, Springer Science & Business Media, 2009.

[10] S. Bandyopadhyay, G. P. Subramanian, R. Foust, D. Morgan, S.-J. Chung, and F. Hadaegh, "A review of impending small satellite formation flying missions," *Proc. of the 53rd AIAA Aerospace Sciences Meeting*, 2015.

[11] J. A. Fax and R. M. Murray, "Information flow and cooperative control of vehicle formations," *IEEE Trans. Autom. Control*, vol. 49, no. 9, pp. 1465-1476, Sep. 2004. [click]

[12] L. Krick, M. E. Broucke, and B. A. Francis, "Stabilisation of infinitesimally rigid formations of multi-robot networks," *International Journal Control*, vol. 82, no. 3, pp. 423-439, Mar. 2009. [click]

[13] F. Dörfler and B. Francis, "Geometric analysis of the formation problem for autonomous robots," *IEEE Trans. Autom. Control*, vol. 55, no. 10, pp. 2379-2384, Oct. 2010. [click]

[14] B. D. O. Anderson, C. Yu, B. Fidan, and J. M. Hendrickx, "Rigid graph control architectures for autonomous formations," *IEEE Control Syst. Mag.*, vol. 28, no. 6, pp. 48-63, Dec. 2008.

[15] Y.-H. Lee, S.-G. Kim, T.-Y. Kuc, J.-K. Park, S.-H. Ji, Y.-S. Moon, and Y.-J. Cho, "Virtual target tracking of mobile robot and its application to formation control," *International Journal of Control, Automation and Systems*, vol. 12, no. 2, pp. 390-398, Apr. 2014. [click]

[16] K.-K. Oh, M.-C. Park, and H.-S. Ahn, "A survey of multi-agent formation control," *Automatica*, vol. 53, no. 3, pp. 424-440, Mar. 2015. [click]

[17] R. Vidal, O. Shakernia, and S. Sastry, "Formation control of nonholonomic mobile robots with omnidirectional visual servoing and motion segmentation," *Proc. of the 2003 IEEE Int. Conf. on Robotics and Automation*, 2003.

[18] P. Renaud, E. Cervera, and P. Martinet, "Towards a reliable vision-based mobile robot formation control," *Proc. of the 2004 IEEE/RSJ Int. Conf. on Intelligent Robots and Systems*, vol. 4, 2004.

[19] L. Vig and J. A. Adams, "Multi-robot coalition formation," *IEEE Trans. Robot.*, vol. 22, no. 4, pp. 637-649, Aug. 2006. [click]

[20] G. L. Mariottini, F. Morbidi, D. Prattichizzo, G. J. Pappas, and K. Daniilidis, "Leader-follower formations: Uncalibrated vision-based localization and control," *Proc. of the 2007 IEEE Int. Conf. on Robotics and Automation*, 2007.

[21] B. Fidan, V. Gazi, S. Zhai, and N. Cen, "Single-view distance-estimation-based formation control of robotic swarms," *IEEE Trans. Ind. Electron.*, vol. 60, no. 12, pp. 5781-5791, Dec. 2013. [click]

[22] R. Siegwart, I. R. Nourbakhsh, and D. Scaramuzza, *Introduction to Autonomous Mobile Robots*, MIT Press, London, England, 2004.

[23] W. Pastorius, "Triangulation sensors: An overview," *INTECH*, vol. 48, no. 7, Jul. 2001.

[24] E. Biyik and M. Arcak, "Gradient climbing in formation via extremum seeking and passivity-based coordination rules," *Proc. of the 46th IEEE Conf. on Decision and Control*, 2007.

[25] M. Zhu and S. Martinez, "An approximate dual subgradient algorithm for multi-agent non-convex optimization," *IEEE Trans. Autom. Control*, vol. 58, no. 6, pp. 1534-1539, Jun. 2013.

[26] K. Sakurama, S. Azuma, and T. Sugie, "Distributed controllers for multi-agent coordination via gradient-flow approach," *IEEE Trans. Autom. Control*, vol. 60, no. 6, pp. 1471-1485, Jun. 2015.

[27] Y. Zhu, S. J. Gortler, and D. Thurston, "Sensor network localization using sensor perturbation," *Proc. of the IEEE INFOCOM*, 2009.

[28] M. Cao, C. Yu, and B. D. O. Anderson, "Formation control using range-only measurements," *Automatica*, vol. 47, no. 4, pp. 776-781, Apr. 2011.

[29] Y.-P. Tian and Q. Wang, "Global stabilization of rigid formations in the plane," *Automatica*, vol. 49, no. 5, pp. 1436-1441, May 2013. [click]

[30] M. Bayat and A. P. Aguiar, "AUV range-only localization and mapping: Observer design and experimental results," *Proc. of the European Control Conf.*, 2013.

[31] B. Jiang, M. Deghat, and B. D. O. Anderson, "Translational velocity consensus using distance-only measurements," *Proc. of the 52nd IEEE Conf. on Decision and Control*, 2013.

[32] B. S. Park and S. J. Yoo, "Adaptive leader-follower formation control of mobile robots with unknown skidding and slipping effects," *International Journal of Control, Automation and Systems*, vol. 13, no. 3, pp. 587-594, Jun. 2015. [click]

[33] A. Loria, J. Dasdemir, and N. A. Jarquin, "Leader-follower formation and tracking control of mobile robots along straight paths," *IEEE Trans. Control Syst. Technol.*, vol. 24, no. 2, pp. 727-732, Mar. 2016. [click]

[34] J. M. Hendrickx, B. D. O. Anderson, J. Delvenne, and V. D. Blondel, "Directed graphs for the analysis of rigidity and persistence in autonomous agent systems," *Int. Jour. of Robust and Nonlinear Control*, vol. 17, no. 10-11, pp. 960-981, Jul. 2007. [click]

[35] J. Cortés, S. Martinez, T. Karatas, and F. Bullo, "Coverage control for mobile sensing networks," *IEEE Trans. Robot. Autom.*, vol. 20, no. 2, pp. 243-255, Apr. 2004. [click]

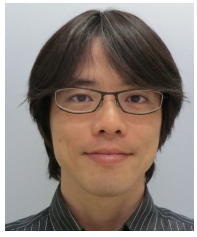

Kazunori Sakurama received the Bachelor's degree in Engineering, the Master's and the Doctoral degrees in Informatics from Kyoto University, Kyoto, Japan, in 1999, 2001, and 2004, respectively. He was an Assistant Professor at the University of Electro-Communications, Tokyo, Japan from 2004 to 2011. He is currently an Associate Professor at Graduate School of Engineering, Tottori University, Tottori, Japan. His research interests include control of multi-agent systems, networked systems and nonlinear systems. He is a member of the IEEE and the Society of Instrument and Control Engineers (SICE).

Yusuke Kosaka received the Bachelor's and Master's degrees in Engineering from Tottori University, Tottori, Japan, in 2014 and 2016, respectively. His research interests include formation control of multi-robots.

Shin-ichiro Nishida received his M.S. and Ph.D. in engineering from Kyoto University. He joined Toshiba Corp. in 1980. His main work was research and development of space robots such as JEMRMS, ETS-VII. He joined National Aerospace Labolatory which is a predecessor of JAXA in 2002. He joined project team of REX-J flight experiment in 2012 as PI. After mission completion of REX-J, he moved to the Tottori University as a professor. His main field of reaserch is about robotics and control systems.